Jurnal Tribologi 29 (2021) 31-40

MYTRIBOS Malaysian Tribology Society

Jurnal Tribologi

Website : jurnaltribologi.mytribos.org e-issn: 2289-7232

Characterization and analysis of AA1100 - SiC_p metal matrix composite fabricated through friction stir processing

Praveen Kumar V. *, Nivetha S.K., Began Peruvazhuthi S., Raman K., Senthil Kumar V.S.

Department of Mechanical Engineering, College of Engineering Guindy Campus, Anna University, Chennai 600025, Tamil Nadu, INDIA.

*Corresponding author: praveenmatceg@gmail.com

KEYWORDS

Aluminum
Metal matrix composite
Friction stir processing
SiC
SEM
Wear

ABSTRACT

In this work, 2 wt.% Silicon Carbide (SiC) particulate reinforced aluminium 1100 (AA1100) Metal Matrix Composite (MMC) was fabricated through Friction Stir Processing (FSP). The average particle size of the SiC used in the present study was analysed using particle size analyser which was found to be 12 μm. The microstructural analysis of base metal and processed samples were carried out with Scanning Electron Microscopy (SEM). Vickers hardness test was carried out at 500 g load with 10 s dwell time. The hardness value of the composite was 52% higher than the base metal. In addition to that, the composite layer has been identified from the hardness test carried out along the depth from top to bottom of the processed plate. The tensile test was performed on MMC which revealed that Ultimate Tensile Strength (UTS) of MMC was 97% higher than the base metal with an increase in stiffness and reduction in strain to failure values. The tribological performance test was carried out with pin on disc tribometer. The wear rate of both the base metal and composite were calculated and it was noted that the wear rate of MMC has decreased by 57% when compared to the base metal. Reduction in wear rate of MMC was attributed to the SiC addition on AA1100 through FSP. Coefficient of Friction vs Time plot indicated lesser frictional force on the MMC surface which implies that SiC in the aluminium matrix acted as a solid lubricant during wear test. Thus, the fabricated AA1100-SiC MMC have high hardness and UTS value with a slight reduction in ductility.

Received 22 December 2020; received in revised form 17 February 2021; accepted 14 April 2021.
To cite this article: Kumar et al., (2021). Characterization and analysis of AA1100 - SiCp metal matrix composite fabricated through friction stir processing. Jurnal Tribologi 29, pp.31-40.

1.0 INTRODUCTION

Metal Matrix Composites are extensively used in the automotive and aerospace components because of their high specific stiffness and strength. The applicant materials need to be less dense and should have high specific strength for their use as structural components (Ashithesh & Kale, 2015). The improvements in density and specific strength are not only the factors of measuring the performance for aerospace materials. Specific dimension of aerospace components is controlled by fatigue crack growth in the structure, durability and also residual stress and corrosion resistance. It is obvious that these composites should be sufficiently reinforced with either fiber or particles (Geeta & Rajesh, 2015). Attempts are made to homogenize the distribution of these reinforcements to obtain isotropic properties. However, when reinforced with fibers the properties are highly heterogeneous (Johanson et al., 2015). Even if alternate layers with different directions are adopted there occurs the problem of delamination (Tanveer et al., 2019). So, to get the uniform structure and property, it is generally advisable to reinforce the matrix with particles (Shankar & Harichandran, 2019). Solid state fabrication of MMCs is gaining attention nowadays. When a material is either processed or fabricated in its solid state, there is a less chance of it to getting trapped with oxide inclusions. In addition to that, the material will be free of voids and defects. In MMCs, which are processed through liquid state, there will be interface and interphase. These interphase products are extremely hard and brittle and function as preferred locations for the crack nucleation and Propagation (Fang et al., 2020 & Carrere et al., 2000). Those produced through solid state means are devoid of these interphase products resulting in safer metallurgical structure.

Friction stir processing evolved from friction stir welding proves to be a promising surface MMCs fabrication method (Mishra et al., 2003 & Sandeep et al., 2018). The method uses a shoulder and a profile pin rotating tool. The material under the tool during FSP undergoes severe plastic deformation due to the intense plastic shearing which is the result of combined action of tool rotation and axial load. This results in the modified finite grain size in the processed nugget zone. The grains formed are all equiaxed and majority of them have high angle grain boundaries. The material is known as interface controlled one since the grain boundary density has been drastically increased. And as a result, increased dislocation motion hindrance increases the material strength. In addition to that, the FSP changes the physical properties of the material without altering the physical condition of the material. This ensures that there is no change of state during the cycle thus resulting in less complexity in carrying out the process with different base metals.

The reinforcement can be added to the base metal through different processes. The most common practice is by cutting a square groove on the metal surface and filling the groove with the reinforcement particles (Ratna, 2016; Puviyarasan & Kumar, 2015; Prasad & Shoba, 2014). After processing, the excess flash is removed immediately. Selection of proper process parameters is necessary to attain defect free composites. Also, tools with variety of pin profiles can been used for FSP process. Some of them are tools with pin profiles such as square, conical, cylindrical, conical threaded, triangular, multi pin etc., The conical pin with threaded profile proves to be an effective one for stirring (powders within matrix) action (García et al., 2016).

The influence of SiC as reinforcement in the mechanical properties and wear characteristics of AA1100 material has not yet been studied in detail. Thus, the present work focuses on the fabrication of SiC particulate reinforced aluminium metal matrix composite through friction stir processing method. The fabricated composite has been characterized and results were discussed elaborately.

2.0 EXPERIMENTAL PROCEDURE

Aluminium 1100 was purchased from the Accurate Metals Industries Private Limited, Mumbai. The composition of the as received material was tested with the spark spectroscopy equipment in order to confirm the material grade. SiC particles were purchased from Shawn Enterprises, Chennai.

Table 1: Composition of aluminium 1100 with % wt of various elements present.

Element	Silicon	Iron	Zinc	Copper	Manganese	Aluminium
% wt	0.283	0.201	0.136	0.15	0.04	Remaining

The composition of AA1100 is mentioned in the Table.1. The reinforcement being chosen was silicon carbide (SiC) particles. As received SiC particle was ball milled with a high energy planetary ball milling equipment to reduce the average particle size. The process was carried out in a stainless-steel vial with tungsten carbide balls. With toluene (2%wt) as process control agent, ball-milling was carried out at 300 rpm for 30 hours. The average particle size of ball milled SiC was determined by laser disperse particle size Distribution Analyzer LA-950.

The base metal plate has the dimensions of 100 mm in length, 70 mm in width and 6 mm in thickness. The tool was made of H13 hardened tool steel and schematic of tool is shown in figure 1. The shoulder has flat face with diameter as 20 mm. The pin has the total length of 5.5 mm with the diameter beneath the shoulder as 6.6 mm and the end diameter as 3.3 mm (conical threaded). The pin has continuous right-hand thread with 1 mm pitch. Friction Stir Processing was performed in a vertical milling machine with constant rotating speed of 900 rpm and traverse speed of 45 mm/min with axial load of 10 kN and tilt angle of 2° and the plunge depth was maintained as 0.4 mm. The FSP procedure is shown in the figure 2.

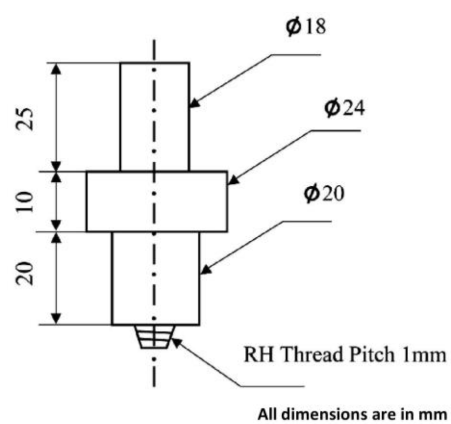

Figure 1: Friction stir tool.

Grooves were cut, with the vertical milling machine, on the vicinity of metal plate to be processed. The groove dimensions were chosen according to the appropriate thickness of Friction stir processed MMC. Groove has the depth of 2 mm and length of 100 mm with 2 mm width. The grooves were cleaned with acetone before powder filling. Using FSP tool without pin, FSP was carried out to close the groove to avoid the spillage of reinforcement particles while preparing the surface composite. The mass of SiC powder filled in the groove was 2.25 g and the weight percentage of SiC in the MMC was calculated as 2 wt.%.

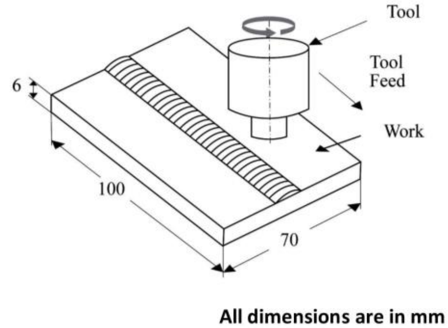

Figure 2: Friction stir procedure.

After FSP, the microstructural analysis of the sample was done using SEM. SEM equipment used in the study was Carl Zeiss MA15/EVO 18 Scanning Electron Microscope. The test sample preparation for SEM analysis was carried out by cutting the material of 10 mm × 10 mm × 5 mm using wire cut electric discharge machining (wEDM). The sample was cut perpendicular to the FSP direction and the cross section of the sample was polished for further examination through SEM. The sample was polished with the grades of emery paper (80, 120, 180, 220, 320, 400, 600, 800, 1000) sheets and then fine polished with disc polisher using diamond paste.

For hardness measurement, sample preparation was performed by cutting the sample of the dimension 20 mm × 6 mm × 5 mm. The sample was then polished using different grades of emery sheets as mentioned earlier followed by disc polishing in order to achieve a mirror finish. Hardness test was carried out across the transverse direction of plate from top to bottom at an interval of 0.5 mm using Bareiss Digi Test Vickers micro-hardness tester. The load was kept at 500 g with the dwell time as 10 s throughout the test. The experiment was repeated for three times for each measurement and the arithmetic mean was taken as correct reading to avoid errors.

Tensile test was performed with Instron Electromechanical 3382A-100 kN equipment. Tensile samples were extracted from the stir zone of processed MMC along the FSP direction. The ASTM E8 tensile specimen line diagram is shown in figure.3. a. Wear test was performed according to ASTM G99-06 using pin on disc tribometer to ascertain the wear characteristics and to analyze the wear mechanism. The test sample was made according to the standard ASTM G99-06 procedure with 6 mm diameter pin and disc was made from EN 31 Steel. The load applied was 10 N and the sliding distance was kept as 1000 m with sliding velocity as 2 m/s. The mass loss of the samples (Base metal and MMC) after the wear test was measured. From that, the wear volume and the wear rate were calculated using eq. 1 and 2 (Jitendra et al., 2016). Extraction of various samples from the processed material are shown in figure 3. b.

$$Wear\ volume = \frac{mass\ loss\ in\ grams}{density} mm^3 \tag{1}$$

$$Wear\ rate = \frac{Wear\ volume}{Applied\ load \times Sliding\ Distance}\ \frac{mm^3}{Nm} \tag{2}$$

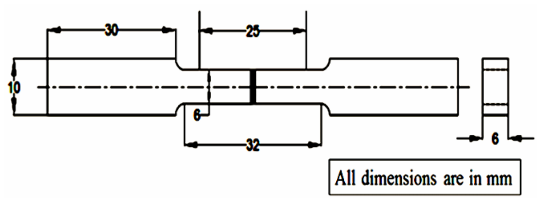

A - Tensile Specimen
B - Microhardness Specimen through thickness of the nugget zone

(a)

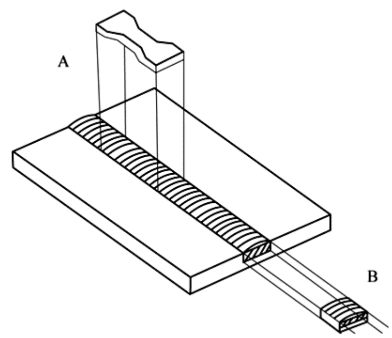

(b)

Figure 3: (a) Tensile Specimen and (b) extraction location of test specimens.

3.0 RESULTS AND DISCUSSION

3.1 Average Particle Size

The Silicon Carbide particles after ball milling has the size distribution which is shown in figure 4. The milled particles have range of diameters and all the particles lie between the size of 0.2976 µm and 37 µm. Fraction of particles were in 1 µm regime and another major fraction was in 10 µm regime. The average particle size was found to be 12 µm. Thus, the reinforcing particles have size ranging from sub-micron to micron level. The narrow size distribution of SiC particulates counteracts the particle fracture in the matrix thus limiting the crack initiation in matrix.

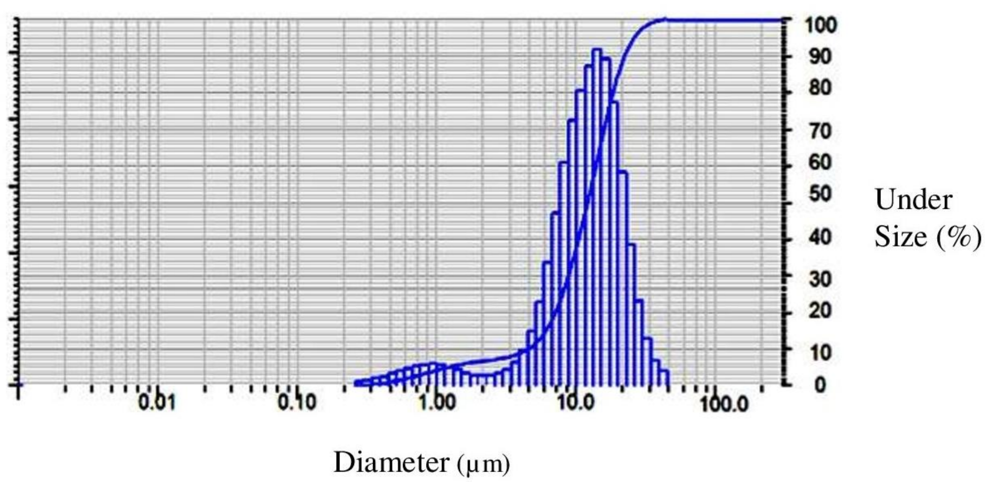

Figure 4: Particle size distribution of ball milled SiC.

3.2 Morphology

The SEM images of both the base metal and MMC are shown in Figures 5.a and 5.b respectively. The presence of intermetallics and oxides were observed in the figure 5.a. The diamond abrasives can be seen in both the images as minute spheroids. From the SEM image of the Friction stir processed MMC sample, the presence of SiC particles on the Al matrix was confirmed. There was no accumulation of SiC abrasive particles in matrix. The silicon carbide particles were distributed evenly in the matrix although minute scratches were visible in both the samples. However, the intermetallics were dissolved greatly due to frictional heat and plastic deformation leading to dynamic recovery and recrystallisation process and only a fraction of them were present in MMC when compared to the base metal. The reinforcing particles were distributed only at the top surface of plate thus the remaining bulk structure has undergone grain refinement and there is an increase in dislocation density due to friction stir processing.

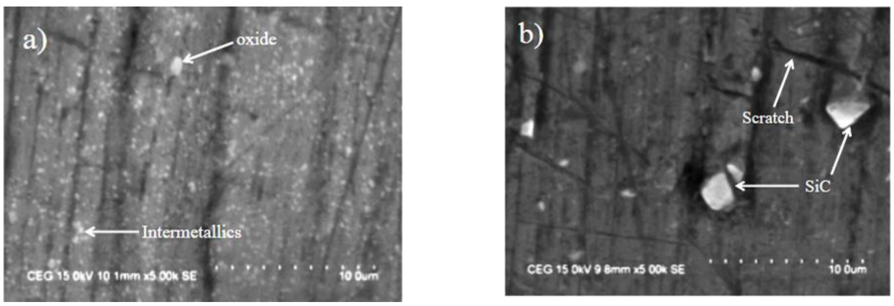

Figure 5: SEM images of (a) base metal and (b) MMC.

3.3 Hardness

The Figure.6 shows the micro hardness profile of the FSPed MMC. The hardness at the near surface is 64 Hv which has decreased along the depth of the sample. The crest hardness is due to reinforcing SiC and grain refinement due to FSP. The strength of the processed sample was attributed to strengthening effect of SiC which hinders the deformation of material (Fang et al., 2020). The Hardness of the base material was found to be 42 Hv. The decrease in hardness along the depth was due to the composite layer. From the SEM images, it was further confirmed and the variations in hardness values across the thickness indicate the presence of composite layer upto 1.5 mm depth from the top surface. The hardness values rarely vary beyond 1.5 mm and the middle portion, which is halfway between the top and bottom surface of plate, has the mean hardness of 55 Hv. However, beyond 4 mm the hardness values fell rapidly as the thermo mechanically affected zones (TMAZ) and heat affected zones (HAZ) are present at bottom of the material.

3.4 Tensile Behavior

The stress strain plots of base metal and MMC is shown in Figure.7. The ultimate tensile strength (UTS) of base metal was 34 MPa and that of the MMC was 67 MPa. The tensile curve of MMC shifts to the right of plot implying that MMC possess higher stiffness than Base metal. The total percentage elongation of base metal was 12.8% and the MMC failed with lesser plastic deformation with total percentage elongation of 6.1%. The strain to failure was reduced greatly indicating that there was a reduction in ductility of MMC which is almost half the value of base metal. The enhancement in UTS was due to the grain refinement and strengthening reinforcement (Anand et al., 2019). Also, the strength increment was attributed to increase in dislocation density due to FSP and the load sharing capability of hard reinforcements (Chawla & Shen, 2001). This prevents the plastic flow of material and the reinforcements act as obstacles aiding dislocation pile up thereby improving the strength. The narrow size distribution of reinforced SiC particulates counteracts the particle fracture in the aluminium matrix when stress is applied thus the load transferring capability between matrix and reinforcement has increased largely thus limiting the crack initiation in the matrix. Overall, the strength and stiffness of composite has been improved through reinforcement (Arnav et al., 2019).

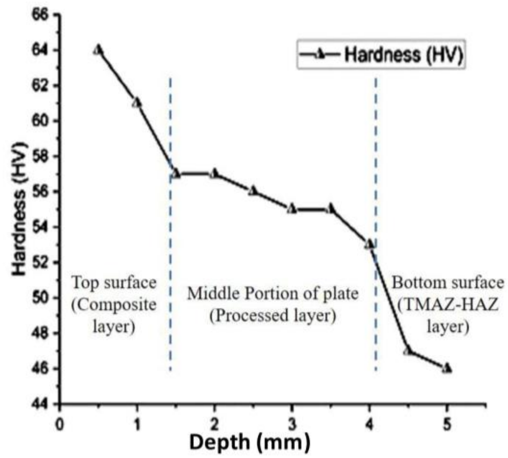

Figure 6: The graph between hardness and depth of MMC.

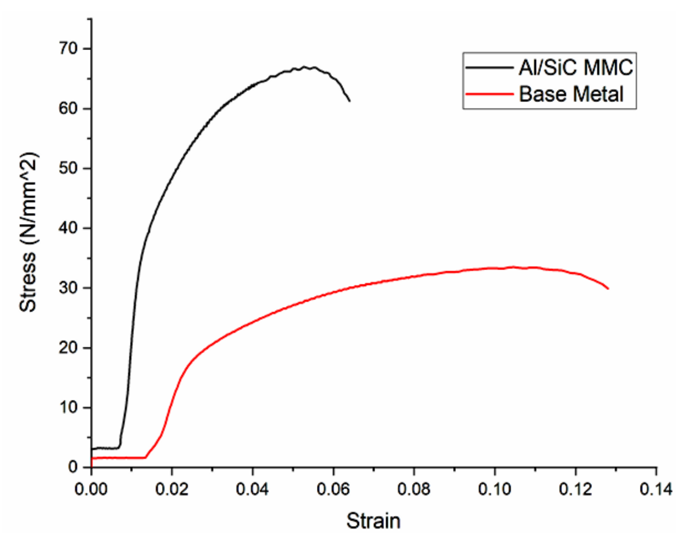

Figure 7: Stress-strain curves of base metal and MMC.

3.5 Wear Analysis

The mass loss and wear rate of both the base metal and MMC are shown in table 2. Both the mass loss and wear rate were high in the case of base material when compared to MMC. The base metal is soft and more ductile than FSPed sample as the grain refinement due to dynamic recovery and recrystallisation has improved the strength of MMC in addition to the effect of hard SiC reinforcements. This has significantly reduced the mass loss in the case of FSPed MMC and thus leading to lower wear rate when compared to the base metal. Also, the hard SiC particles in the matrix reduced the surface contact between pin and disc as these SiC particles protruding out after the matrix worn out (Jingming et al., 2014). Thus, the shearing load was predominantly taken up by particles thus reducing wear. This also reduces the adhesion of debris on the surface of material.

Table 2: Mass loss and wear rate of Base metal and MMC.

Sample	**Before (g)**	**After (g)**	**Mass loss (g)**	**Wear volume (mm^3)**	**Wear rate $\times 10^{-5}$ (mm^3 / Nm)**
Base	0.4408	0.3594	0.0814	0.3018	3.0761
MMC	0.4178	0.3851	0.0327	0.1212	1.2354

The graph between co-efficient of friction (COF) and sliding time is shown in Figure 8. The friction coefficient of MMC is less than the base metal indicating lesser frictional force on the surface of MMC. The fluctuations in COF of Friction stir processed material are high and the value of COF decreases momentarily which is attributed to crack growth and slip deformation beneath the surface in the material (Alan, 2015). The hard reinforcements thus acted as solid lubricant reducing wear on MMC (Jagatheeshwaran et al., 2016 & Praveen, 2017).

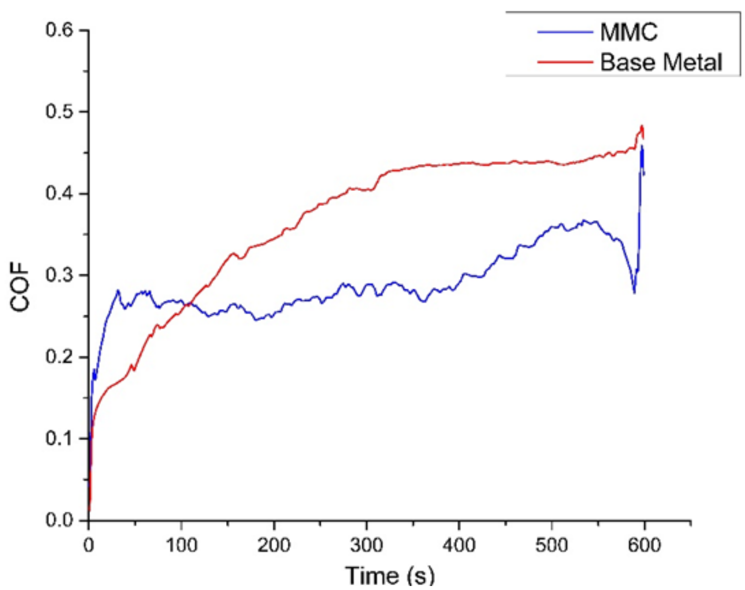

Figure 8: Graph between friction co-efficient and time of base metal and MMC.

4.0 CONCLUSIONS

The defect free composite has been fabricated through solid state FSP method. The microstructure of both the base metal and MMC has been observed through SEM which revealed the presence of SiC in processed material confirming the homogeneous distribution of SiC in aluminum matrix.

The improvement in hardness of the MMC is found to be varying along the depth confirming the composite layer at the top owing to high hardness values which is 40.5% higher than base metal hardness and relatively less hardness at higher depth revealing the stir zone of processed metal followed by TMAZ and HAZ.

The ultimate tensile strength of the composite is found to be twice that of the base metal with reduction in the ductility of composite almost by half the value of base metal with only 6.1% total elongation compared to base metal which has total % elongation of 12.8%.

Wear analysis revealed that the improvement in hardness and grain refinement in processed material resulted in reduced mass loss and a massive reduction in wear rate of composite by 40% than base metal and during the wear test, the reinforcement acted as solid lubricant on the mating surface.

Thus, the fabricated Al/SiC metal matrix composite could be a choice of material that would serve as secondary structures in body frame and as sheets in the hood of automobiles and as secondary support structures in body frame of aircrafts.

ACKNOWLEDGEMENT

The authors would like to acknowledge that the work was presented at ITRS 2020 with abstract ID ITRS002.

REFERENCES

Alan Hase, Mizuta Kazuho, Nishizawa Yukio, Sugimoto Koji, Okayama Katsuya. (2015). Visualization and Evaluation of Friction and Wear Phenomena for Brake Pads Using In Situ Observation and Acoustic Emission Measurement Method. EuroBrake conference 2015, EB2015-FID-004.

Anand Singh Rathaur, Jitendra Kumar Katiyar, Vinay Kumar Patel (2019) Experimental analysis of mechanical and structural properties of hybrid aluminium (7075) matrix composite using stir casting method. IOP Conference Series: Mater. Sci. Eng. 653 012033.

Arnav Shil, Sandipan Roy, Balaji, P. S., Jitendra Kumar Katiyar, Sumit Pramanik, Anuj Kumar Sharma. (2019). Experimental analysis of mechanical properties of stir casted aluminium graphene nanocomposites. IOP Conference Series: Mater. Sci. Eng. 653 012021.

Ashithesh, V. C., Kale. (2015). Aluminium based metal matrix composites for aerospace application: A Literature Review. IOSR-JMCE, 12, 31-36

Carrere, N., Martin, E., & Lamon, J. (2000). The influence of the interphase and associated interfaces on the deflection of matrix cracks in ceramic matrix composites. Composites Part A: Applied Science and Manufacturing, 31(11), 1179-1190.

Chawla, N., Shen, Y. L. (2001). Mechanical behavior of particle reinforced metal matrix composites. Advanced engineering materials, 3(6), 357-370.

Fang Guangwu, Li Long, Gao Xiguang, Song Yingdong (2020) Finite Element Analysis of the Crack Deflection in Fiber Reinforced Ceramic Matrix Composites with Multilayer Interphase Using Virtual Crack Closure Technique. Applied Composite Materials, 27, 307–320.

García-Bernal, M. A., Mishra, R. S., Verma, R., & Hernández-Silva, D. (2016). Influence of friction stir processing tool design on microstructure and superplastic behavior of Al-Mg alloys. Materials Science and Engineering: A, 670, 9-16.

Geeta Agnihotri & Rajesh Purohit. (2015). Advanced aluminium matrix composites: The critical need of automotive and aerospace engineering fields. Materials today: proceedings, 2, 3032-3041.

Jagatheeshwaran, M. S., Elayaperumal, A., & Arulvel, S. (2016). The role of calcinated sea shell particles on friction-wear behavior of electroless NiP coating: fabrication and characterization. Surface and Coatings Technology, 304, 492-501.

Jingming Tanga, Yifu Shena & Junping Lia (2019) Influences of friction stir processing parameters on microstructure and mechanical properties of SiC/Al composites fabricated by multi-pin tool. Journal of Manufacturing Processes, 38, 279-289.

Jitendra K. Katiyar, Sujeet K. Sinha, Arvind Kumar. (2016). Effects of carbon fillers on the tribological and mechanical properties of an epoxy-based polymer (SU-8), Tribology - Materials, Surfaces & Interfaces, 10:1, 33-44.

Johanson, K., Harper, L. T., Johnson, M. S., & Warrior, N. A. (2015). Heterogeneity of discontinuous carbon fibre composites: Damage initiation captured by Digital Image Correlation. Composites Part A: Applied Science and Manufacturing, 68, 304-312.

Mishra, R. S., Ma, Z. Y., & Charit, I. (2003). Friction stir processing: a novel technique for fabrication of surface composite. Materials Science and Engineering: A, 341(1-2), 307-310.

Parveen Kumar, Wani, M. F. (2017). Friction and wear behaviour of hypereutectic Al-Si alloy/steel tribopair under dry and lubricated conditions. Jurnal Tribologi 15, 21-49.

Prasad, D. S., & Shoba, C. (2014). Hybrid composites–a better choice for high wear resistant materials. Journal of Materials Research and Technology, 3(2), 172-178.

Puviyarasan, M., & Kumar, V. S. (2015). An Experimental Investigation for Multi-Response Optimization of Friction Stir Process Parameters During Fabrication of AA6061/B 4 C p Composites. Arabian Journal for Science and Engineering, 40(6), 1733-1741.

Ratna Sunil, B. (2016). Different strategies of secondary phase incorporation into metallic sheets by friction stir processing in developing surface composites. Materials Engineering, 11, 12.

Sandeep Rathee, Sachin Maheshwari, Arshad Noor Siddiquee, Manu Srivastava. (2018). Distribution of reinforcement particles in surface composite fabrication via friction stir processing: Suitable strategy. Materials and Manufacturing Processes, 33, 239-261.

Shankar, S., & Harichandran, S. (2019). Aluminium alloy reinforced with fly ash: Techniques and particle size. Jurnal Tribologi, 23, 13-37.

Tanveer Ahmed Khan, Hoon Kim, Hyun-Joong Kim . (2019). Fatigue delamination of carbon fiber-reinforced polymer-matrix composites. Failure Analysis in Biocomposites, Fibre-Reinforced Composites and Hybrid Composites, 1-28.